Temperature and composition dependence of the Soret coefficient in Lennard-Jones mixtures presenting evaporation/condensation phase transition

Erminia Leonardi,[1,a)] Bruno D'Aguanno,[1] and Celestino Angeli[2]

[1]*CRS4, Center for Advanced Studies, Research and Development in Sardinia, Parco Scientifico e Tecnologico, POLARIS, Edificio 1, 09010 Pula (CA), Italy*
[2]*Dipartimento di Chimica, Università di Ferrara, Via Borsari 46, I-44100 Ferrara, Italy*

The thermodiffusive behavior of a Lennard-Jones binary mixture has been studied by using nonequilibrium molecular dynamics. In particular, the dependence of the Soret coefficient, S_T, on the temperature and composition has been investigated, exploring a wide range of temperatures from 1000 K to the condensation temperature of the mixture. In a previous paper the dependence of S_T on the temperature and the composition was studied for Lennard-Jones binary mixtures presenting mixing/demixing (consolute) phase transition, and the results allowed the formulation of a very simple expression with the computed values of S_T in the one phase region outside the critical region closely fitted by the function $[T - T_c(x_1)]^{-1}$, with $T_c(x_1)$ the demixing temperature of the mixture under study. The results of the present work show that the same expression of S_T can be found for the one phase region outside the evaporation/condensation region but now with T_c representing the condensation temperature of the mixture under study. © *2011 American Institute of Physics*.
[doi:10.1063/1.3561672]

I. INTRODUCTION

Thermodiffusion, also known as Soret effect,[1,2] is the phenomenon in which a mass flux in a mixture is induced by a temperature gradient. It is a nonequilibrium effect which describes the coupling between a temperature gradient and an induced resulting mass flux, which adds up to the Fickian flux, in a multicomponent system. The presence of a constant temperature gradient induces the development of a concentration gradient, whose amplitude at the steady state is controlled by the Soret coefficient, $S_T = D_T/D$ (D and D_T are the Fickian and the thermal diffusion coefficients, respectively).

Assuming fluxes and gradients in the z-direction, in a binary mixture at the steady state one has[3]

$$S_T = \frac{D_T}{D} = -\frac{1}{x_1(1-x_1)}\left(\frac{\partial x_1}{\partial z}\right)\left(\frac{\partial T}{\partial z}\right)^{-1}, \quad (1)$$

where x_1 is the molar fraction for the species 1 (commonly chosen as the heavier species). Positive values of S_T indicate that species 1 tends to accumulate in the "cold" region.

The complete description of the relevant properties of the thermodiffusion process is out of the scope of the present work, and the reader is referred to recent reviews[4,5] and to two papers of our group[6,7] for more details. A study previously published by our group[7] is of particular interest for the present work and the main results there obtained are therefore here briefly recalled. In Ref. 7 the dependence of S_T on the temperature has been investigated by varying the value of the term ϵ_{12} of the Lennard-Jones (LJ) interaction potential of a binary mixture of Argon and Krypton. The study was carried out by using nonequilibrium molecular dynamics, where the temperature gradients were generated following the method proposed by Müller-Plathe.[3,8] In summary, in this method the energy flux is generated by exchanging in the simulation box, for each species, the velocity vectors of the hottest particle in the "cold" region with the coldest one in the "hot" region. This leads to an energy transfer from the cold region to the hot one if the coldest particles of the hot region has less kinetic energy than the hottest one of the cold region (due to the broad form of the Maxwell–Boltzmann distribution this hypothesis is normally satisfied). As a consequence of this artificial energy flux, a temperature gradient develops between the hot and the cold regions, until a steady state is reached, in which the energy flux due to the temperature difference compensates the artificial flux. The velocity exchange is done every N_{exch} simulation time steps, where N_{exch} is chosen (in a trial and error strategy) so that the temperature gradient is as small as possible with the constraint to show a clear (and numerically stable) concentration gradient. This method has been implemented in our laboratory into the commercial code M.Dynamix,[9] and is adopted also in the present study (see also Refs. 6 and 7 for the details of the implementations of this algorithm in our calculations). The key result obtained in Ref. 7 is that the Soret coefficient diverges at the demixing temperature of the mixture following the simple relation $S_T = [T - T_c]^{-1}$, where T_c is the demixing temperature (depending on the composition of the mixture). The divergence of S_T when T approached T_c is well known. Indeed, by considering the critical temperature, T_c, as a reference, one can identify two regions. In the first region (called critical domain, usually few Kelvin, or less, around T_c) the divergence of the

correlation length of the fluctuations leads to universal scaling laws for the critical behavior of the transport coefficients.[10] While D_T does not show a critical behavior, D presents the characteristic asymptotic (Ising-like) critical slowing down[11] approaching T_c, leading to an asymptotic divergence of the Soret coefficient like $(T - T_c)^{-0.67}$ (see for instance Refs. 12 and 13). The second region, situated outside the critical region, is characterized by the fact that the relevance of the fluctuations becomes vanishing, the correlation length is smaller than the characteristic length scale and the behavior is not universal, showing a marked dependence on the nature of the interacting details (classical mean field, or van der Waals, regime). In 2004 Enge and Köhler[13] indicated, for the classical mean field regime, the scaling $S_T \simeq \varepsilon^{-1}$, where $\varepsilon = (T - T_c)/T_c$. This result is obtained starting from the long wavelength limit of the collective diffusion coefficient, considering the thermal activated nature of the background part (the one surviving in the classical mean field regime) of D and D_T and supposing that both the background contribution of the Onsager coefficient (α^{b}) and D_T have a similar activation energy $k_B T_a$. The $(T - T_c)^{-1}$ behavior has been experimentally confirmed[11,13] for a polymer blend for large values of ε. It is important to note that this result indicates a scaling behavior and not the absolute amplitude of the effect. The importance of the simple relation found in Ref. 7 comes from the fact that it is a complete equation (and not just a power-low scaling relation), that it is valid over a broad range of temperature (of the order of many hundreds of kelvin), and, obviously, from its simplicity (depending only on one property of the mixture).

The aim of this work is to further proceed in this research project, by presenting a study concerning the evaluation of the dependence of S_T on the temperature in the case of a binary LJ mixture in a range of temperatures ending on the line of evaporation/condensation critical points (liquid–vapor equilibrium).

While the P–T phase diagram of a single component system shows a single critical point, the critical behavior of a binary mixture is, by far, much more complex. In fact, the phase diagram region of a binary mixture in which critical phenomena are occurring is characterized by four critical points and by transition lines joining such points. There are two critical points, say CP_1 and CP_2, corresponding to the critical points of the pure components and two critical points, say CEP_1 and CEP_2, corresponding, respectively, to the critical end points of the liquid–vapor and the liquid–liquid critical lines. If, for example, the points CP_1 and CEP_1 are linked by a liquid–vapor critical line, the points CP_2 and CEP_2 will be linked by a critical line along which two different critical transitions are observed. By starting from the CP_2 point, the critical line first describes a liquid–vapor critical transition which is then followed by a liquid–liquid critical transition (this last part of the critical lines is known as the critical consolute line). Finally, the points CEP_1 and CEP_2 are linked by a critical line which indicates the three-phase equilibrium (coexistence of two liquid phases and a vapor phase). Clearly, in the P–T representation of the thermodynamic phase diagram, the multiphases coexistence is just represented by transition lines. The description of critical phenomena of binary mixtures in the

TABLE I. Lennard-Jones parameters for Argon and Krypton (from Ref. 3).

Atom(type)	m (amu)	σ (Å)	ε (kJ/mol)
Kr(1)	83.80	3.633	1.39
Ar(2)	39.95	3.405	1.00

P–T phase diagram is well illustrated in literature.[14–16] In the present work, the line starting from the critical point CP_2 is followed (liquid–vapor equilibrium) until a point in which the critical line starts to describe a vapor–vapor equilibrium (before ending in the critical point CEP_2). This second part of the critical line has been the subject of the analysis performed in Ref. 7.

The rest of the paper is organized as follows: in Sec. II the computational details of the simulations are described, in Sec. III the results of the present study are reported, and in Sec. IV some conclusive remarks are given.

II. COMPUTATIONAL DETAILS

All simulations have been performed with 1500 atoms interacting through Lennard-Jones potentials, defined as

$$U_{ij}^n (r_{ij}) = 4\epsilon_{ij} \left[\left(\frac{\sigma_{ij}}{r_{ij}} \right)^{12} - \left(\frac{\sigma_{ij}}{r_{ij}} \right)^6 \right]. \qquad (2)$$

In this equation σ_{ij} is the distance at which the potential changes sign, ε_{ij} is the depth of the potential, and r_{ij} is the distance between particles i and j.

The parameters of the like interactions, σ_{11}, ε_{11}, σ_{22}, and ε_{22}, are reported in Table I for the sake of completeness, and they refer to those of Krypton (species 1) and Argon (species 2).[3] The interaction potential between unlike species is computed using the Lorentz–Berthelot mixing rule

$$\sigma_{12} = (\sigma_1 + \sigma_2)/2,$$
$$\epsilon_{12} = \sqrt{\varepsilon_{11}\varepsilon_{22}}. \qquad (3)$$

The results of the calculations are here reported following the law of the corresponding states (only approximate for multicomponent systems), which enables, for a given transport property, to uncouple the thermodynamics state contribution from the molecular parameter.[17] For a mixture of LJ spheres, the reduced thermodynamics variables are

$$T^* = \frac{k_B T}{\varepsilon_x}, \; \rho^* = \frac{N\sigma_x^3}{V}, \; \text{and} \; P^* = \frac{P\sigma_x^3}{\varepsilon_x}, \qquad (4)$$

where k_B is the Boltzmann constant, N is the number of particles, V is the volume, and P is the pressure. The parameters ε_x and σ_x are computed following the van der Waals one fluid approximation[18]

$$\sigma_x^3 = \sum_{i=1}^{2} \sum_{j=1}^{2} x_i x_j \sigma_{ij}^3, \qquad (5)$$

$$\varepsilon_x \sigma_x^3 = \sum_{i=1}^{2} \sum_{j=1}^{2} x_i x_j \varepsilon_{ij} \sigma_{ij}^3. \qquad (6)$$

The simulation box is an orthorhombic periodic cell of size $L^* \times L^* \times 3L^*$, where $L^* = L/\sigma_x$ is the reduced length, chosen equal to 8.51. Such cell has been divided into $N_s = 12$ slabs of equal thickness, orthogonal to the z-direction. Slab 0 is defined as the "cold" slab and slab $N/2$ as the "hot" slab. Because of the symmetry of the simulation box, average values of temperature and composition are calculated between slab $(N_s/2) - i$ and $(N_s/2) + i$, with $i = 1, 5$, having excluded the first (0) and central (6) slabs because of the unphysical effects they can present due to the particle exchange procedure. The time step Δt is 1 fs and the chosen cutoff distance, $r_c^* = 4.23$, corresponds to an energy truncation, E_c of the order of 10^{-4} kJ/mol. Standard long range correction to the Lennard-Jones potential is also considered in the calculations. Simulations have been performed in the canonical ensemble (NVT), with temperature control by means of the Nose–Hoover thermostat.[19, 20]

The nonequilibrium molecular dynamics (NEMD) simulation, on which statistic information is collected, is always performed after two runs. The first one is an equilibrium molecular dynamics (EMD) simulation 2×10^6 time steps long and the second one is a NEMD simulation, other 2×10^6 time steps long. In this way we are sure that the system in the final NEMD simulation is at the steady state. This assumption has been verified by analyzing the behavior of the time evolution of the total energy and of the temperature and composition profiles, which is expected to be constant during the final NEMD simulation. In the final NEMD calculation, data are collected over a simulation 14×10^6 time steps long.

The temperature used in the EMD simulation represents the temperature around which the temperature gradient develops, that is, a sort of average temperature in the NEMD steps. This temperature is indicated in the following with T_{eq}^*. NEMD simulations have been performed at a series of values of T_{eq}^*, with the aim to cover a wide range of temperatures (from about 60 to 1000 K) and to have the Soret coefficient as a function of the temperature. The value of N_{exch} depends on T_{eq}^*: it is equal to 1200 for $T_{eq}^* = 0.837$ (120 K), to 700 for $T_{eq}^* = 1.744$ and 1.953 (250 and 280 K, respectively), and to 500 for $T_{eq}^* = 2.791$, 4.186, and 5.581 (400, 600, and 800 K, respectively).

A detailed description of the procedure for the calculation of the Soret coefficient from the concentration and temperature profiles is given in Refs. 6 and 7. In summary, starting from the analytic fitting of the temperature and of the composition on a set of z^* values (corresponding to the center of each slab of the simulation box), Eq. (1) allows the definition of $S_T^* = S_T \varepsilon_x / k_B$ for each value of z_i^* (the center of slab i) through the analytic derivatives with respect to z^* of $T^*(z^*)$ and $x_1(z^*)$. One can thus obtain S_T^* for each couple $T^* \left(z_i^* \right)$ and $x_1 \left(z_i^* \right)$ in the ranges $T_{max}^* - T_{min}^*$ and $x_1^{max} - x_1^{min}$, where T_{max}^* and T_{min}^* (x_1^{max} and x_1^{min}) are the maximum and minimum temperature (molar fraction) found in the various slabs. It can be demonstrated that, if S_T^* has the form $(T^* - \tilde{T}^*)^{-1}$ (that actually found in the simulations described in details in Ref. 7 and hereafter) and the temperature profile is linear in z (as always found in our simulations), then the
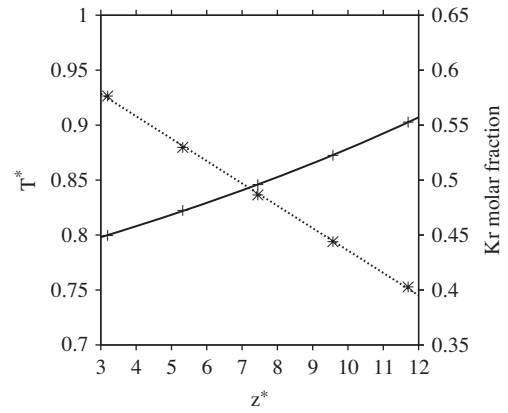

FIG. 1. Temperature (dotted line and $*$ symbols) and composition profiles (full line and $+$ symbols) for the equimolar mixture of Argon and Krypton at $T_{eq}^* = 0.837$. The fitting parameter of $x_1(z^*) = 1/(a + bz^*)$ are $a = 2.378$ and $b = -0.0485$ [root mean square of the residuals (RMS) = 0.0004] while for the temperature, $T^*(z^*) = c + dz^*$, $c = 0.990$, and $d = -0.0204$ [RMS = 0.0019].

concentration profile assumes the form

$$x_1(z^*) = \frac{1}{a - bz^*}. \tag{7}$$

This expression has been used to fit the x_1 values computed in the NEMD simulations.

It is worth noticing that Eq. (1) is valid in the frame of the linear nonequilibrium thermodynamics, where it is postulated that the fluxes depend linearly on the generalized forces.[21] However, from the integration of this equation one obtains that $x_1(z)$ is not a linear function of z even if S_T is constant and $T(z)$ is a linear function of z. Therefore, there is no reason to expect a linear composition profile in the NEMD simulations. This aspect is discussed in Ref. 6 to which the reader is referred for more details.

III. NEMD RESULTS

In the range of temperatures explored in our simulations, the concentration profiles are always well fitted with the function reported in Eq. (7), as shown, for instance, in Fig. 1 for the case of the NEMD simulation of the equimolar LJ mixture at $T_{eq}^* = 0.837$.

A series of NEMD simulations has been performed with $x_1 = 0.1$, 0.5, and 0.9, and, for each one of these compositions, a wide range of temperatures T_{eq}^* has been spanned, thus obtaining the dependence of S_T^* on T^*.

In the range of temperatures explored and for each mixture considered, S_T^* always has positive values, it increases as the temperature is lowered, and finally it diverges, following a behavior that is well described by the fitting function $S_T^* = 1/(T^* - \tilde{T}^*)$.

In order to better understand the physical meaning of the temperature $\tilde{T}^*$ at which the Soret coefficient diverges, equilibrium molecular dynamics simulations have been performed on a wide range of temperature around $\tilde{T}^*$.

The phase stability of the mixture has been investigated in terms of the infinite wavelength limit $k \to 0$ of the Bhatia–Thornton, BT, structure factors $S_{CC}(k)$, $S_{NN}(k)$, and
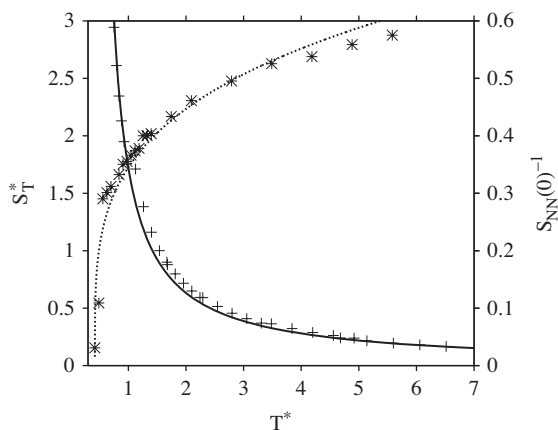
FIG. 2. Soret coefficient, S_T^* (full line and + symbols), and inverse of the structure factor, S_{NN}^{-1} (dotted line and * symbols), vs T^* for an equimolar mixture of Lennard-Jones particles.

$S_{NC}(k)$,[22] which, in the form derived from the Ornstein–Zernike equations for a binary mixture, can be written as[23,24]

$$S_{CC}(k) = 1 + n x_1 x_2 [\tilde{h}_{11}(k) + \tilde{h}_{22}(k) - 2\tilde{h}_{12}(k)],$$

$$S_{NN}(k) = 1 + n[x_1^2 \tilde{h}_{11}(k) + x_2^2 \tilde{h}_{22}(k) + 2x_1 x_2 \tilde{h}_{12}(k)],$$

$$S_{NC}(k) = n x_1 x_2 [x_1 \tilde{h}_{11}(k) - x_2 \tilde{h}_{22}(k) + (x_2 - x_1)\tilde{h}_{12}(k)], \quad (8)$$

where n is the total number density, $\tilde{h}_{\alpha\beta}(k)$ is the Fourier transform of the correlation function $h_{\alpha\beta}(r) = g_{\alpha\beta}(r) - 1$, and $g_{\alpha\beta}(r)$ is the radial distribution function.

By knowing that the BT structure factors express the correlations of the total number density and composition fluctuations, a thermodynamic stability matrix can be constructed, and the precise combination of fluctuations which diverge at $k = 0$ can be determined.[15,25] For the investigated systems here presented, the incoming divergences in the BT structure factors, S_{NN}, correspond to a pure evaporation–condensation (E/C) phase transition.

At this point it must be stressed that the vapor–liquid phase transition represents an important property which is very sensitive to the intermolecular interactions. In order to
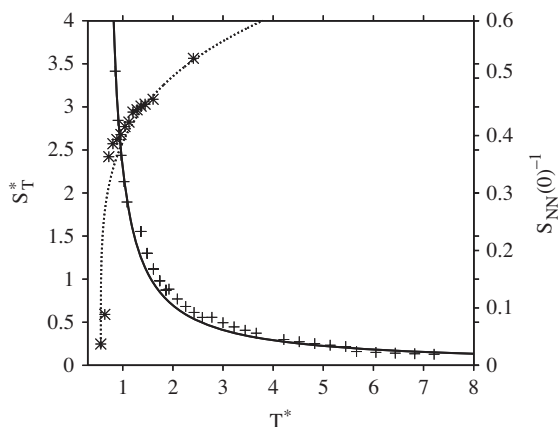

FIG. 3. Soret coefficient, S_T^* (full line and + symbols), and inverse of the structure factor, S_{NN}^{-1} (dotted line and * symbols), vs T^* for the LJ mixture with $x_1 = 0.1$.
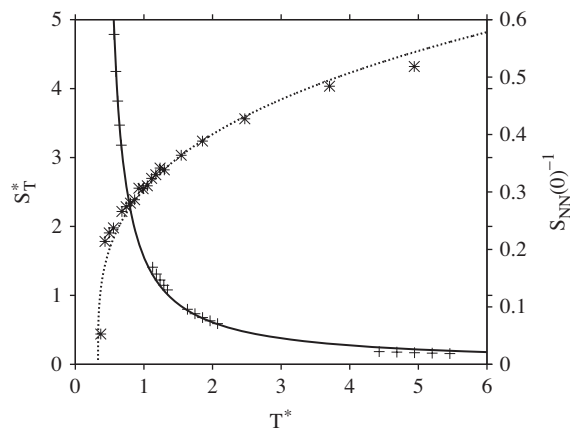

FIG. 4. Soret coefficient, S_T^* (full line and + symbols), and inverse of the structure factor, S_{NN}^{-1} (dotted line and * symbols), vs T^* for the LJ mixture with $x_1 = 0.9$.

correctly calculate the E/C phase transition for a Ar/Kr mixture, with x_1 varying from 0 to 1, the Lennard-Jones potentials are not adequate[26] and correct calculations should employ accurate two-body potentials. Moreover, contributions from three-body dispersion interactions resulting from third-order multipole terms should be also considered, given that vapor–liquid equilibria are affected by these terms.[27–30] For these reasons the calculated E/C transition temperatures here reported are not in strict agreement with the experimental values for actual Ar/Kr mixtures. In addition, it is worth noticing that the strategy here adopted is not well suited for the accurate calculation of phase transitions, which are better described in the grand canonical ensemble. Nevertheless, the aim here is only to have an indication of a possible phase transition with an estimation of the temperature at which it happens and not to precisely compute it.

The calculated values of the inverse of the structure factor, $S_{NN}(0)^{-1}$, at various T^* have been fitted by the function $c/(T^* - T_c^*)^b$, where T_c^*, b, and c are fitting parameters. As already found in the case of a mixing/demixing phase transition of LJ binary mixtures,[7] the divergence of both the structure factor and the Soret coefficient happens at temperatures very close to each other. Such behavior is clearly shown in Figs. 2–4 for the mixtures corresponding to $x_1 = 0.5, 0.1$, and 0.9, respectively, where both S_T^* and $S_{NN}(0)^{-1}$ are plotted as function of the reduced temperature.

A series of EMD simulations on a wide range of temperatures has been also performed for systems corresponding to pure species, and the divergences of their structure factors have been compared with those of the mixtures with $x_1 = 0.1$ and 0.9, respectively. From the simulation results we find that the mixture with $x_1 = 0.1$ presents a phase transition E/C at $T^* = 0.56$ (70 K), which can be compared with a value of 0.63 (75 K) obtained for $x_2 = 1$. Similarly, the LJ mixture with $x_1 = 0.9$ presents a E/C phase transition at $T^* = 0.33$ (53 K), which can be compared with the value of 0.36 (58 K) of the pure species with $x_1 = 1$.

The plots of $S_{NN}(0)^{-1}$ versus T^*, corresponding to the pure species, are shown in Fig. 5. Moreover, the values of $\tilde{T}^*$ and T_c^* at different mixture compositions are indicated in
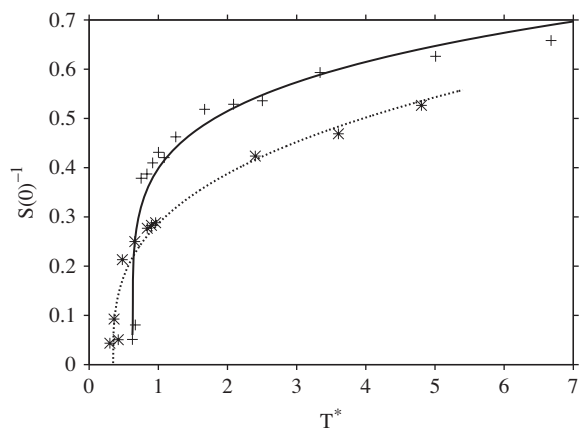
FIG. 5. Inverse of the structure factor, $S(0)^{-1}$, vs T^* for the pure components, $x_1 = 0$ (full line and $+$ symbols) and $x_1 = 1$ (dotted line and $*$ symbols).

Tables II and III, respectively. From these results we can conclude that S_T^* and S_{NN} diverge to the same temperature, and this allows us to express the Soret coefficient as

$$S_T^*\left(T^*\right) = \frac{1}{T^* - T_c^*}, \tag{9}$$

where T_c^* is the boiling temperature of the mixture.

This dependence of S_T^* on T^* confirms the key result of our previous study on LJ mixtures presenting mixing/demixing phase transitions. Indeed, Eq. (9) was also found in Ref. 7, with the only difference that T_c^* is there the mixing/demixing temperature. As already noted in Ref. 7, we want to stress that

- only one characteristic property of the mixture (the critical temperature associated to a phase transition) is involved in a very simple relation, with a clear connection with the expression $S_T = T^{-1}$ valid for ideal gas mixtures;
- Eq. (9) is not simply a power-law scaling relation, as those discussed in Ref. 7 for the cases of mixtures close to the critical temperature[12,31] and in the classical mean field regime,[13] but a complete equation that allows the calculation of the Soret coefficient once T_c is known;
- Eq. (9) is valid over a broad range of temperatures (of the order of many hundreds of K).

The two latter aspects does not hold for instance for the scaling rule[12,31] connecting S_T with the critical temperature, T_c,

TABLE II. Dependence of the Soret coefficient on the temperature at different values of x_1. Values of the fitting parameter $\tilde{T}$ for the various values of x_1. The analytic fitting function is $S_T^* = 1/(T^* - \tilde{T}^*)$. RMS is root mean square of the residuals.

x_1	$\tilde{T}^*$	RMS
0.1	0.5641 ± 0.0068	0.12
0.5	0.4186 ± 0.0059	0.09
0.9	0.3564 ± 0.0014	0.05

TABLE III. Dependence of the inverse of the structure factor, $S_{NN}^{-1}(0)$ on the temperature at different values of x_1. Values of the fitting parameter T_c for the various values of x_1. The analytic fitting function is $S_{NN}^{-1}(0) = c/(T^* - T_c^*)^b$. RMS is root mean square of the residuals.

x_1	T_c^*	RMS
0.0	0.6259 ± 0.0056	0.06
0.1	0.5621 ± 0.0012	0.06
0.5	0.4185 ± 0.0067	0.04
0.9	0.3304 ± 0.0179	0.03
1.0	0.3460 ± 0.0206	0.04

that is only valid in a close interval around T_c (inside the critical domain).

IV. CONCLUSIONS

The thermodiffusion process in a Lennard-Jones binary mixture has been investigated for three different mixture compositions. In particular, besides the equimolar mixture, mixtures rich in each one of the two components ($x_1 = 0.1$ and 0.9) have also been considered. The Soret coefficient has been calculated, by means of NEMD simulations, on a wide range of temperatures up to the condensation point of the system, whose value has been determined from the analysis of the phase stability of the system. This investigation has been done calculating the dependence of the structure factor, $S_{NN}(0)$, on the temperature, and finding for which value of the temperature it diverges. The comparison between the divergence of the structure factor and of the Soret coefficient has allowed to identify the divergence of S_T with the evaporation/condensation phase transition. The interpolation of the results of the NEMD simulations has led to a very simple relationship, $S_T^* = \left[T^* - T_c^*\right]$, between the Soret coefficient and the condensation temperature of the mixture. Besides its simplicity and wide applicability (it is valid over a large interval of temperature and for different mixture compositions), this relationship is of particular interest given that a similar expression for S_T has been found in a previous study[7] on LJ mixture presenting mixing/demixing (consolute) phase transition (T_c being in this case the mixing/demixing temperature).

In the opinion of the authors, these two studies on model systems (spherical particles interacting through LJ potentials) should stimulate the application of the presented methodology to other interaction potentials in order to gain a deeper thermodynamic understanding of the dependence of S_T on the critical phenomena from a general point of view. Work in this direction is in progress.

[1]C. Ludwig, Sitzungsberichte der Kaiserlichen Akademie der Wissenschaften, Mathematisch-Naturwissenschaftliche Klasse **20**, 539 (1856).
[2]C. Soret, Arch. Sci. Phys. Nat. **3**, 48 (1879).

[3] D. Reith and F. Müller-Plathe, J. Chem. Phys **112**, 2436 (2000).

[4] K. I. Morozov, Phys. Rev. E **79**, 031204 (2009).

[5] K. Harstad, Ind. Eng. Chem. Res. **48**, 6907 (2009).

[6] E. Leonardi, B. D'Aguanno, and C. Angeli, J. Chem. Phys. **125**, 054507 (2008).

[7] E. Leonardi, B. D'Aguanno, and C. Angeli, J. Chem. Phys. **132**, 124512 (2010).

[8] F. Müller-Plathe, J. Chem. Phys. **106**, 6082 (1997).

[9] A. P. Lyubartsev and A. Laaksonen, Comput. Phys. Commun. **128**, 565 (2000); M.DynaMix—a scalable portable parallel MD simulation package for arbitrary molecular mixtures.

[10] J. Luettmer-Strathmann, Lect. Notes Phys. **584**, 24 (2002).

[11] A. Voit, A. Krekhov, and W. Köhler, Phys. Rev. E **76**, 011808 (2007).

[12] M. Giglio and A. Vendramini, Phys. Rev. Lett. **34**, 561 (1975).

[13] W. Enge and W. Köhler, Phys. Chem. Chem. Phys. **6**, 2373 (2004).

[14] M. A. Anisimov, E. E. Gorodetskii, V. D. Kulikov, and J. V. Sengers, Pis'ma Zh. Eksp. Teor. Fiz. **60**, 522 (1994); JETP Lett. **60**, 535 (1994).

[15] L. Strigari, M. Rovere, and B. D'Aguanno, J. Chem. Phys. **105**, 2020 (1996).

[16] A. Deerenberg, J. A. Schouten, and N. J. Trappeniers, Physica A **101**, 459 (1980).

[17] J. P. Boon and S. Yip, *Molecular Hydrodynamics* (Dover, New York, 1991)

[18] J. P. Hansen and I. R. McDonald, *Theory of Simple Liquids* (Academic Press, London, 1986).

[19] S. Nose, J. Chem. Phys. **81**, 511 (1984).

[20] G. W. Hoover, Phys. Rev. A **31**, 1695 (1985).

[21] S. R. de Groot and P. Mazur, *Non-equilibrium thermodynamics* (North-Holland, Amsterdam, 1962).

[22] A. B. Bhatia and D. E. Thornton, Phys. Rev. B **2**, 3004 (1970).

[23] B. D'Aguanno and C. Nardone, Nuovo Cimento **16**, 1205 (1994).

[24] G. Malescio, Phys. Rev. A **42**, 2211 (1990).

[25] X. S. Chen and F. Forstmann, J. Chem. Phys. **97**, 3696 (1992).

[26] G. Marcelli and R. J. Sadus, J. Chem. Phys. **111**, 1533 (1999).

[27] A. Z. Panagiotopolous, N. Quirke, M. Stapleton, and D. J. Tildesley, Mol. Phys. **63**, 527 (1988).

[28] R. J. Sadus and J. M. Prausnitz, J. Chem. Phys. **104**, 4784 (1996).

[29] J. A. Anta, E. Lomba, and M. Lombardero, Phys. Rev. E **55**, 2707 (1997).

[30] R. J. Sadus, Fluid Phase Equilib. **144**, 351 (1998).

[31] L. Mistura, Il Nuovo Cimento B **12**, 35 (1972).